JOURNAL OF MATERIALS SCIENCE **38** (2003) 4587–4596

Influence of the HVOF spraying process on the microstructure and corrosion behaviour of Ni-20%Cr coatings

M. E. AALAMIALEAGHA, S. J. HARRIS*, M. EMAMIGHOMI
School of Mechanical, Material, Manufacturing Engineering and Management, University of Nottingham, UK; Department of Metallurgy, University of Tehran, Iran
E-mail: sam.harris@nottingham.ac.uk

The microstructure and the aqueous corrosion resistance of coatings produced by High Velocity Oxy-Fuel (HVOF) spraying techniques has been investigated. Two types of spraying processes have been employed i.e., Topgun HVOF using propylene gas and Met-Jet II HVOF with kerosene liquid fuel together with two forms of Ni-20%Cr powders i.e., water and inert gas atomised. The oxide, porosity and the amount of melted material in the coatings were characterised using scanning electron microscopy (SEM) and X-ray diffraction (XRD), whilst the corrosion resistance of the coatings and the ability to protect the underlying mild steel substrate was evaluated by use of a salt spray chamber and potentiodynamic tests.

MetJet II produced coatings from gas-atomised powder with a lower oxide content, a reduction in porosity and less melted material, as the residence time of particles in the combusted gas stream was shortened. Water atomised powder formed a higher volume fractions of unmelted material and porosity when compared with gas-atomised powder coatings. This was encouraged by the presence of a thin oxide layer, which formed during the production of the water-atomised powder. The orientation of oxides and pores in the coatings had a major effect on their aqueous corrosion behaviour. Better protection for the underlying steel substrate (>3000 h exposure in a salt spray test) was obtained with the coating produced from the gas-atomised powder with the MetJet II system, which had the lowest porosity/oxide content running perpendicular to the substrate surface. The major factor in preventing attack on the mild steel substrate is the amount of interconnecting porosity which allows the corrodant to percolate through the coating.

1. Introduction

High Velocity Oxy-Fuel (HVOF) spray techniques can produce high performance alloy and cermet coatings for applications that require wear resistant surfaces. Recently liquid fuel has been introduced as an alternative to gaseous fuels, thus improving energy density in the combustion process in the HVOF system. This permits the transfer of higher levels of kinetic energy to powder particles injected into the combusted gas stream and this promotes the possibility of denser coatings [1, 2]. HVOF coatings require the careful matching of the powder feed material to the process variables e.g., fuel type, fuel/oxygen ratio, together with the design and geometry of the spray gun. These variables influence the temperature and velocity of the particles in the combusted gas stream and thus the energy of impact on the substrate [1]. The point of injection of powder and the geometry of the combustion chamber in HVOF systems can have a major role on the thermal energy transferred from the hot gases to the particles and thus the amount of molten material and oxide produced during coating [3, 4].

The corrosion resistance of nickel alloy coatings produced by gas fuelled HVOF systems has been investigated by previous workers [5–7], and they have demonstrated that the coatings are not as resistant as the bulk alloys to aggressive acid solutions. Furthermore it is necessary to seal the coatings with a polymer to prevent ingress of these aggressive corrodants to an underlying carbon steel substrate. In the deposition of a Ni-Cr alloy by HVOF, it is desirable to control microsegregation of the alloy in order to limit the redistribution of the chromium, e.g., by limiting the formation of oxides.

The oxide formation in nickel-chromium alloys is highly sensitive to the chromium content, as well as the temperature and the oxygen content of the combusted gas [8]. The main types of oxides that form on the surface of nickel-chromium alloys are nickel oxide (NiO),

*Author to whom all correspondence should be addressed.

chromium oxide (Cr_2O_3), and a spinel oxide of nickel and chromium i.e., $NiCr_2O_4$ [9, 10]. The amount and type of oxide may depend on the conditions that exist in the spray gun system and in the freejet as the combustion gas emerges from the nozzle and is exposed to ambient conditions.

The aim of this paper is to investigate the oxide content, porosity level and the amount of melting produced during the formation of gas and liquid fuelled HVOF coatings from two different types of powder (gas and water atomised); and how this relates to the corrosion properties of coatings exposed to aggressive conditions.

2. Experimental

2.1. Coating materials and spraying systems

Two types of Ni-20%Cr alloy powder, i.e., gas (G) and water atomised (W) were used (see Table I) to spray onto mild steel substrates in the form of $25 \times 50 \times 2$ mm thick sheet coupons. Two spray guns were employed: (i) a Topgun system with a gaseous propylene fuel (GF) and (ii) A Met-Jet II system which had a liquid fuel (kerosene) (LF) supply, they operated under conditions specified in Table II. The powders were fed parallel to the gas stream and entered into the combustion chamber of the Topgun system whilst the powder was radially fed at the entrance to the barrel in the MetJet II system.

The richness in oxygen, R, specified in Table II relates to the oxygen/fuel ratio, a, and the stoichiometric condition which is based on sufficient oxygen being available in the combustion chamber for complete combustion of the fuel.

$$a = \frac{\eta \text{ oxygen}}{\eta \text{ fuel}} \tag{1}$$

where η is the number of moles, thus

$$R = a/a_o \tag{2}$$

where a_o is the ratio for stoichiometric combustion; with $R < 1$ the gas mixture is lean in oxygen and $R > 1$ it is rich in oxygen.

2.2. Characterisation of coatings

A JEOL 6400 scanning electron microscope (SEM) was used to provide images of powder and coatings obtained in secondary electron (SE) and back scattered electron (BSE) conditions. To study the distribution of the oxides and porosity in the coatings, backscatter images (BSE) of polished cross sections and plan views of the coatings were examined. As wavelength dispersive X-ray spectrometry (WDX) provided better resolution of the oxygen peak, a JEOL-JSM 35C microscope equipped with a wavelength dispersive spectrometer determined the oxygen content of the coatings. Calibration of the WDX detector was carried out using a zirconia (ZrO_2) sample, and initial tests counts were made on a known mixture of FeO and Cr_2O_3 and other standards.

An X-ray diffraction (XRD) technique was used to identify the crystal structure of the feedstock powder and coating samples. This was carried out in a SEIMENS D 500 machine, equipped with a DACO-MP multiprocessor controller and DIFFRAC-AT-V3.0 software for processing the results. To quantify the oxide contents of the coatings, powder samples of the known oxides were used to provide an internal standard. The standards contained varying amount of NiO, Cr_2O_3, and $NiCr_2O_4$, and were prepared for XRD analysis in a mixture with the original Ni-20%Cr powder. From the data obtained on these standards the oxide content of each coating was calculated assuming that each oxide was present in its stoichiometric composition.

A major factor in providing an alloy that is resistant to aqueous corrosion is associated with the need for it to have a homogeneous single phase. Different thermal histories for the original powders together with those

TABLE I Powder composition (wt%) and size

	Ni	Cr	Si	Mn	Fe	Co	C	Particle size (μm)
Gas atomised powder (G)	77.10	20.04	0.87	1.33	0.10	0.06	0.10	16–44
Water atomised powder (W)	79.40	19.17	0.90	0.10	0.33	0.06	0.01	16–44

TABLE II Spraying conditions for Topgun and MetJet II systems

Topgun					
Test type	Oxygen flow rate (m^3/min)	Propylene flow rate (m^3/min)	Richness in oxygen (R)	Type of powder atomisation	Stand off distance (m)
GFG	0.216	0.066	0.73	Gas	0.25
GFW	0.226	0.056	0.89	Water	0.25
MetJet II					
Test type	Oxygen flow rate (g/sec)	Kerosene flow rate (g/sec)	Richness in oxygen (R)	Type of powder atomisation	Stand off distance (m)
LFG	21.04	5.61	1.08	Gas	0.35
LFW	21.04	5.61	1.08	Water	0.35

experienced during spraying can promote degrees of inhomogeneity i.e., with presence of cored dendritic microstructures. The cored dendrites were detected by etching the samples in a mixture of 3 parts hydrochloric acid (37%) to 1 part nitric acid (69%) and they were observed by optical microscope and SEM.

Salt spray tests to BS 7479-1991-(ISO 9227-1990) were used to evaluate the presence of networks of open porosity in the coatings, which permitted an attack on the underlying substrate. Electrochemical measurements, i.e., anodic potentiodynamic sweeps, were also employed to demonstrate the passive and active behaviour of the coating in a 0.5 M sulphuric acid solution. This was carried out to ASTM G5-87 specifications with 0.5 M sulphuric acid solution deaerated with nitrogen at 30°C. An ACM Gil 8AC potentiostat was used to perform the tests at a sweep rate of 20 mV/min over a 1500 mV range.

3. Results

3.1. SEM analysis of powders and coatings

SEM/WDX analysis was carried out on a cross section of the powder particles. BSE images revealed some different microstructures in water and gas atomised powders, see Fig. 1. In the gas-atomised case there was a cored dendrite structure in virtually all particles. As far as water-atomised powders were concerned there were only a few dendrite structures which were formed in the larger particles. In small particles, <30 μm, the structures were more featureless with some evidence of a grain size of <10 μm.

Under a reduced acceleration voltage, the WDX result demonstrated that the oxygen level near the surface of water atomised powder was $\sim$0.7 wt%, whilst at the centre of the particle a value close to 0.2 wt% was obtained. On a cross section of a gas atomised powder particle the oxygen level was $\sim$0.1% in the near surface region. The thickness of the coatings produced by Topgun and MetJet II were in the range 275 ± 25 μm.

Cross-sections of coatings produced from gas-atomised powder in the unetched condition were examined in the SEM; their images showed the presence of inter-splat dark oxide stringers running parallel to the substrate surface in MetJet II coatings, whilst both inter- and intra-splats oxides existed randomly in coatings produced by Topgun, see Fig. 2. The sizes of the splats were very different in the two coatings. The liquid fuel coatings had splats which were $\sim$20 μm thick, whilst those in the Topgun coating had thickness values which were <5 μm. Some of the porosity ran perpendicular to the substrate surface and this was more prevalent in the gas fuelled coatings.

WDX analysis for oxygen content was obtained on both Topgun and MetJet II coatings produced from each powder type. The results shown in Table IV demonstrate a significantly higher oxygen content in the Topgun coatings. The difference between oxygen content for the coatings produced from the two different powders was much smaller.

3.2. Unmelted materials

The presence of unmelted and partially melted material was revealed in etched cross-sections of coatings in Figs 3 and 4. The gas fuelled Topgun produced coatings from gas atomised powder with more evidence of melting (Fig. 3a) that was the case with liquid fuelled MetJet II (Fig. 3b). This may be deduced from the retention of cored dendrites (as seen in the powder) in each coating. Melted material appeared in a structureless form since it had undergone faster cooling. In the coatings produced from water atomised powder there was less evidence of cored dendrites, see Fig. 4a and b, due to the absence of dendritic patterns in this form of powder.

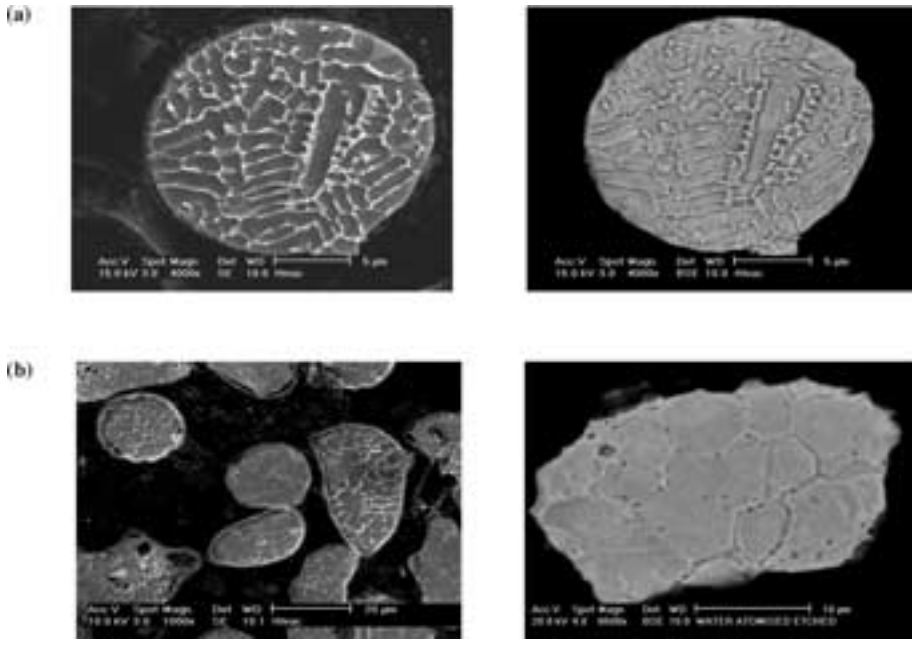

Figure 1 SE and BSE images of etched cross-section of (a) gas-atomised and (b) water-atomised powder.

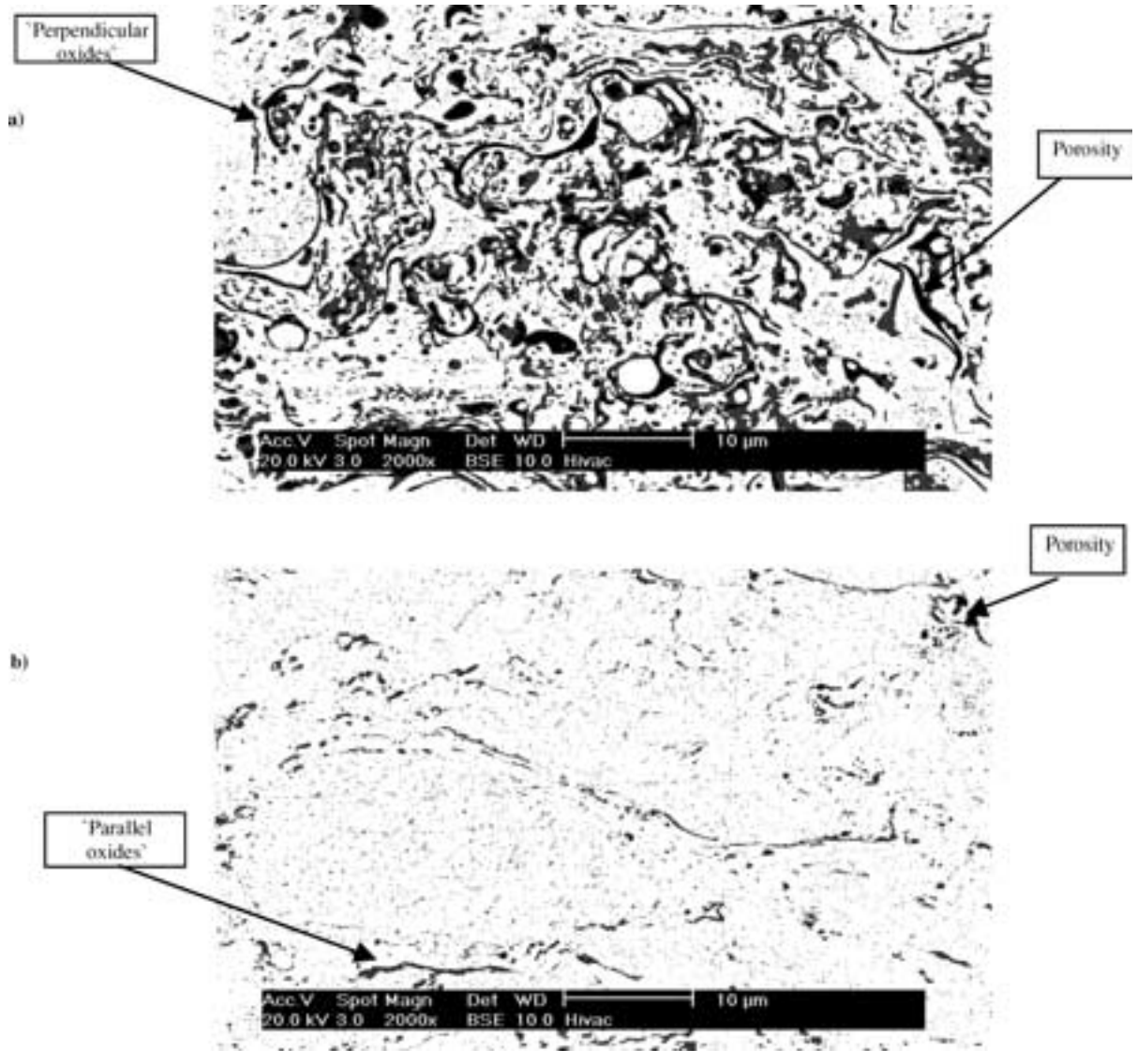

Figure 2 Cross-sections of coatings produced by (a) gas fuelled Topgun and (b) liquid fuelled MetJet II using gas atomised powder. The Topgun coating contains greater amounts of oxide and porosity.

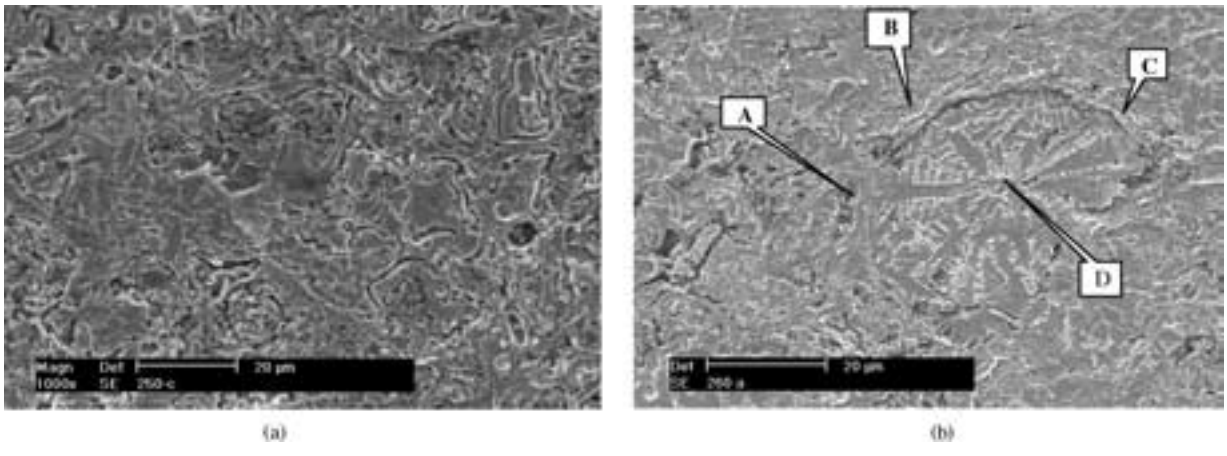

Figure 3 SE images of etched coating sections produced from gas atomised powder showing: (a) smaller regions of unmelted and partially melted particles produced in Topgun gas fuelled spraying (GFG1). (b) small fully melted area A, oxide B, partially melted area C and larger unmelted particle D produced by MetJet II liquid fuel spraying (LFG2).

3.3. Porosity

The porosity level in coating produced with the liquid fuel MetJet II system was lower than that in the sprayed coating obtained from the Topgun gaseous fuel system, see Table III . Minimum porosity (i.e., 0.4%) is obtained in the coating produced from gas-atomised powder and sprayed with the MetJet II whilst a higher porosity of more than 4% is formed in the coating produced from

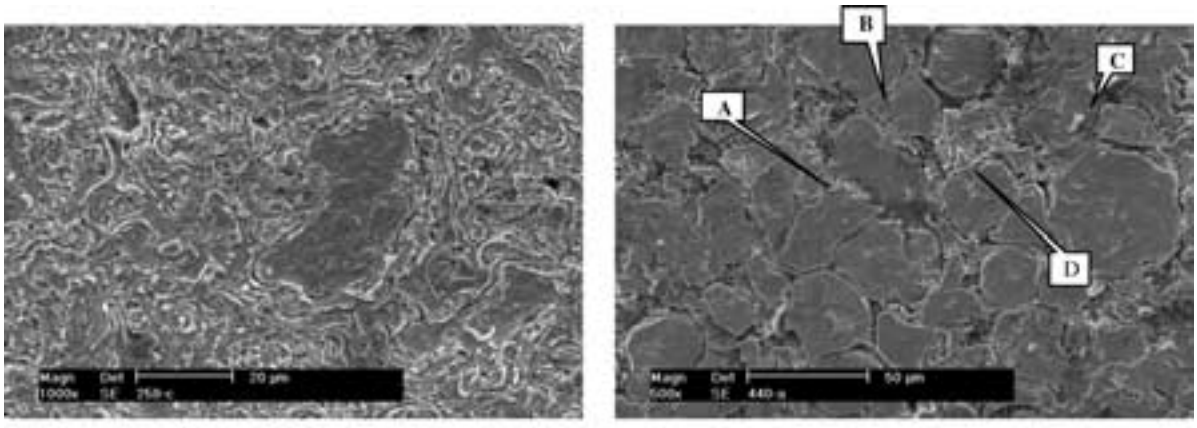

Figure 4 SE images of etched coating sections produced from water atomised powder showing limited evidence of the degree of melting when sprayed by (a) Topgun or (b) MetJet II. The amount of melting was difficult to determine as the dendritic patterns were absent from the powder which was used. Evidence of fully melted (A), oxide (B), partially melted (C) and unmelted particle (D) areas are given in (b).

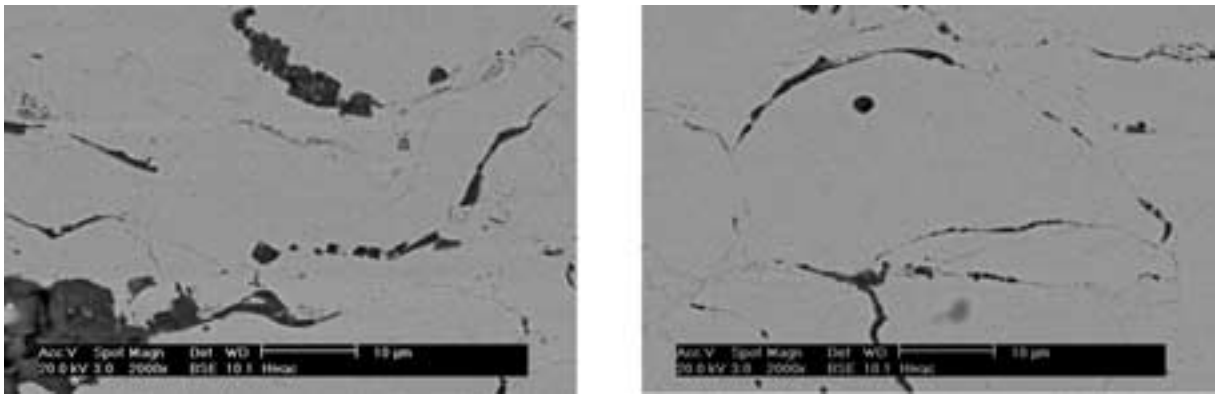

Figure 5 Dome-shaped splats shown in a SEM BSE micrograph of a cross-section of a coating (LFW2) produced by a MetJet II gun using water-atomised powder. With less melting the splats had changed from being flat leticular shapes to dome shaped.

water-atomised powder using the Topgun. In water-atomised powder coatings porosity is higher in comparison with the gas-atomised powder coatings. Fig. 5 shows the form of the porosity in a liquid fuel coating produced from water-atomised powder i.e., with porosity existing at inter-splat boundaries. Porosity levels and distributions depend upon the amount of liquid phase present and the kinetic energy of the particles in flight. Less liquid reduces the shrinkage porosity whilst high kinetic energy induces solid particle deformation that closes up pores between particles.

3.4. X-ray diffraction

To obtain a measurement of the quantity of each oxide present in the coating an Internal Standard method was employed. By correlating the integrated intensity e.g., $I_{Cr_2O_3}$ from the diffractometer trace for each oxide in mixtures of oxides and alloy with known weight percentages of oxide, a calibration curve for each oxide was produced, see Fig. 6. Using these calibration curves the weight% of each oxide e.g., $W_{Cr_2O_3}$ in each coating can be deduced from the data represented in Fig. 7a and b, and this is given in Table IV.

These results demonstrate that the stronger presence of oxides in the Topgun coatings correlate with oxygen contents found by SEM/WDX also given in Table IV. Of the three oxides, NiO is present in greater amounts in all coatings with the exception of the MetJet II coating produced from water-atomised powder. The traces plotted in Fig. 7 effectively demonstrate the increase in oxide content (all three forms) produced in the spray process.

TABLE III Porosity in coatings

Coating type	%Porosity
GFG	2.1
GFW	4.2
LFG	0.4
LFW	1.6

3.5. Corrosion resistance

A ranking sequence was obtained from the salt spray test, which used two methods of assessing corrosion behaviour. Corrosion was prevented at the edges of the sample by protecting them with a stopping off treatment. The corrosion products observed were from the underlying steel substrate. The first method of assessment was to specify the time to the first observed rust spot and the second was to measure the % area taken over by rusting after 2000 h exposure, see Table V.

TABLE IV Weight% of each oxide in each coating based on XRD data using the internal standard method and WDX analysis

Coating type	$W_{(NiCr)}$	W_{NiO}	$W_{Cr_2O_3}$	$W_{NiCr_2O_4}$	Total oxide content (wt%)	wt%O_2 by XRD	wt%O_2 by WDX
GFG	96.1	2.7	0.4	0.8	3.9	0.9	1.0
GFW	96.6	2.5	0.4	0.5	3.4	0.8	1.3
LFG	97.3	2.0	0.2	0.5	2.7	0.6	0.4
LFW	98.9	0.2	0.5	0.4	1.1	0.3	0.3

Observations made on the coating sections remaining after the test did reveal the existence of pores and oxides but not in any significantly greater amount that was present in the as sprayed coating. There was no major evidence of corrosion at the surface of the coating and no effective reduction in coating thickness had taken place.

The gas-atomised powder sprayed by the MetJet II system provided the superior coating (LFG) with the

TABLE V Observations made on the samples exposed to the salt spray test

Coating type	Time for the first sign of corrosion (h)	The % of total area corroded after 2000 h
LFW	3	25
GFG	36	80
GFW	120	18
LFG	>3000	0

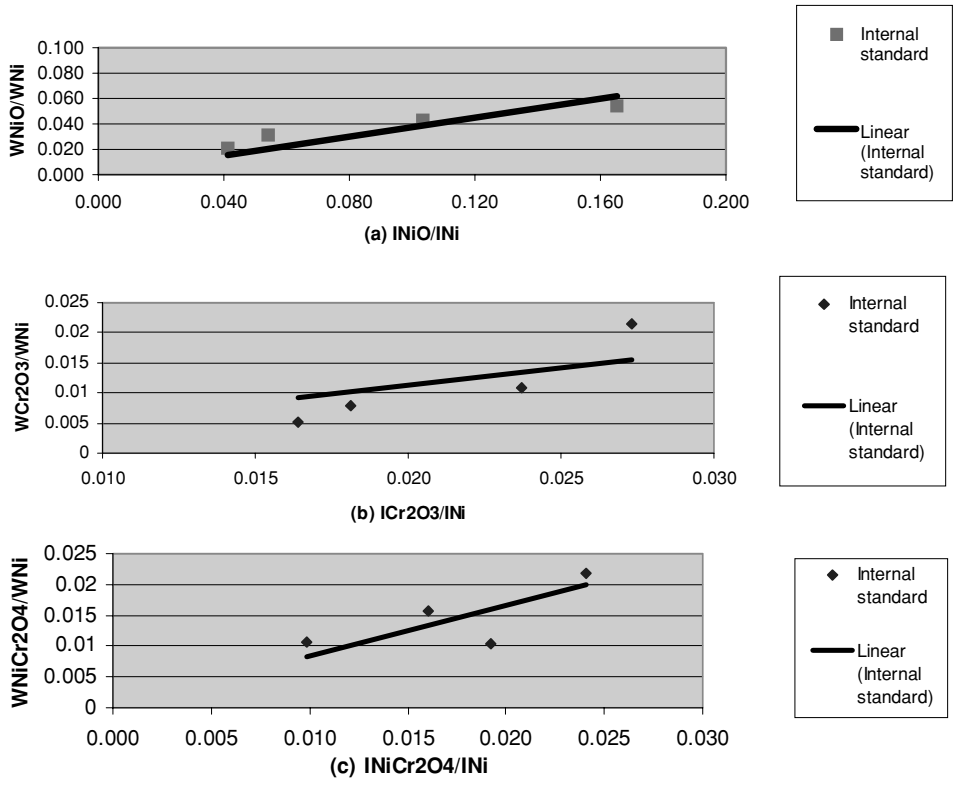

Figure 6 Weight ratio oxide to metal e.g., W_{NiO} to W_{Ni} plotted against integrated intensity ratio oxide to nickel e.g., $I_{Cr_2O_3}$ to I_{Ni} for the three oxides NiO, Cr_2O_3 and $NiCr_2O_4$ mixed with known amounts of the alloy.

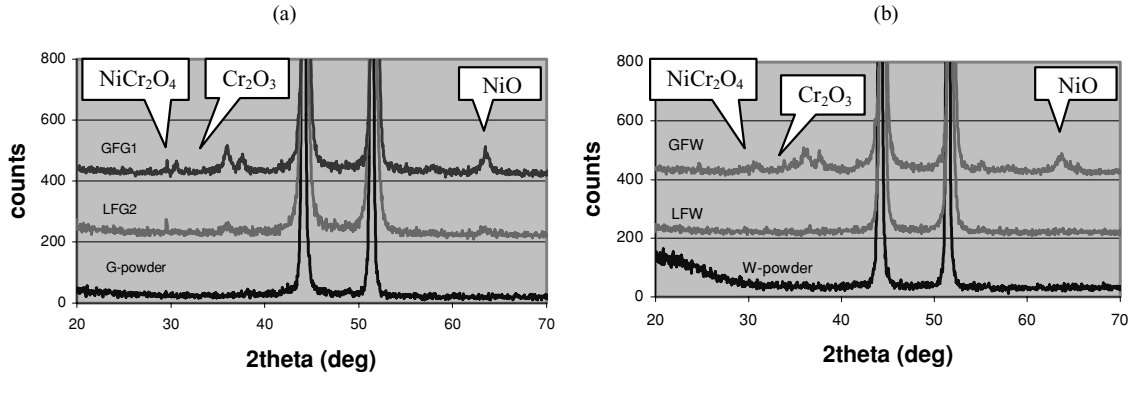

Figure 7 XRD intensity counts for the oxides found in powder and in sprayed coatings over the 2theta range 20° to 70°: (a) gas atomised powder and related coatings and (b) water atomised powder and related coatings.

TABLE VI Results obtained from potentiodynamic test on coatings

Coating type	GFG	GFW	LFG	LFW
Passive current density (mA/cm^2)	∼0.5	∼0.1	∼0.05	∼0.4
Rest potential (mV) vs. SCE	−283	−295	−291	−295
Flade potential (mV) vs. SCE	+810	+286	+589	+275

longest exposure time (>3000 h) before any sign of substrate corrosion appeared in the salt spray test. This same spray system produced a coating (LFW) with water-atomised powder, which gave the shortest corrosion time (3 h) before rust was observed, see Table V. With water-atomised powder the gaseous fuel Topgun system produced a better coating (GFW), resisting the onset of corrosion for 120 h. Although the GFG coating resisted initial corrosion for 36 h, the area of the coating affected after 2000 h was much greater than with any other coating. This would suggest the coating had been severely undermined and this expanded the area of corroded steel.

Electrochemical measurements revealed that the passive current density for a Topgun coating (GFG) in a potentiodynamic test in 0.5 M sulphuric acid was an order of magnitude greater than one sprayed by MetJet II (LFG) when sweeping in the anodic direction, see Fig. 8. The rest potentials for both coatings produced from gas-atomised powder were approximately the same. These observations would suggest that the intrinsic corrosion resistance of this MetJet II coating itself was superior to that of the Topgun coating. The passive current density of a water atomised powder coating produced by Topgun and MetJet II systems were 0.1 and 0.4 mA/cm^2 respectively which appears to reverse the intrinsic resistance of the gas-atomised powder coatings.

4. Discussion

4.1. Influence of combustion products on oxidation behaviour

In the combustion of propylene (C_3H_6) and kerosene ($C_{12}H_{26}$) in oxygen it is necessary to consider eight combustion products, which may be determined by an analysis based on the 'progress of reaction approach' [11] for thermodynamic equilibrium conditions using an appropriate computational algorithm. From this approach the temperature and oxygen content of the flame can be calculated, see Table VII. This demonstrates a much higher availability of oxygen (O_2 + O) in the combusted gas stream in the MetJet II gun (13.9 wt%) and also a higher flame temperature (3166 K) than was the case in the Topgun (7.1 wt% and 3081 K). This would suggest that oxidation might occur more rapidly during coating formation when using the MetJet II system.

4.2. Amount of oxide in coatings produced by the gas and liquid fuel systems

Coatings sprayed by the two different systems revealed that the MetJet II coatings had a lower level of oxide present when compared with those from Topgun irrespective of whether gas or water atomised powder was used. This is demonstrated in Table IV, which give amounts of oxygen and oxide in the coating as measured by SEM/WDX and Internal Standard XRD methods. The reduction in oxide content which occurred with liquid fuel spraying of gas-atomised Ni-20%Cr powder related to all types of oxide i.e., NiO, Cr_2O_3 and spinel. With the water-atomised powder the same is true except for the Cr_2O_3 content (LFW). However, this reduction in oxide content does not relate to the availability of oxygen in the combusted gas or the predicted high flame temperature, see Table VII. Because the predicted high combustion temperature in MetJet II is reduced in the barrel at the convergent-divergent nozzle, this leads to an increase in gas velocity and a reduction in gas temperature. All of this occurs prior to the radial injection of the powder into the barrel. Hence, the powder temperature is reduced for two reasons i.e., a shorter time for heat transfer as the particle velocity is raised by the faster moving gas and a lower gas temperature.

In Fig. 2 it is noticeable that the distribution of oxide is very different in the MetJet II and Topgun coatings.

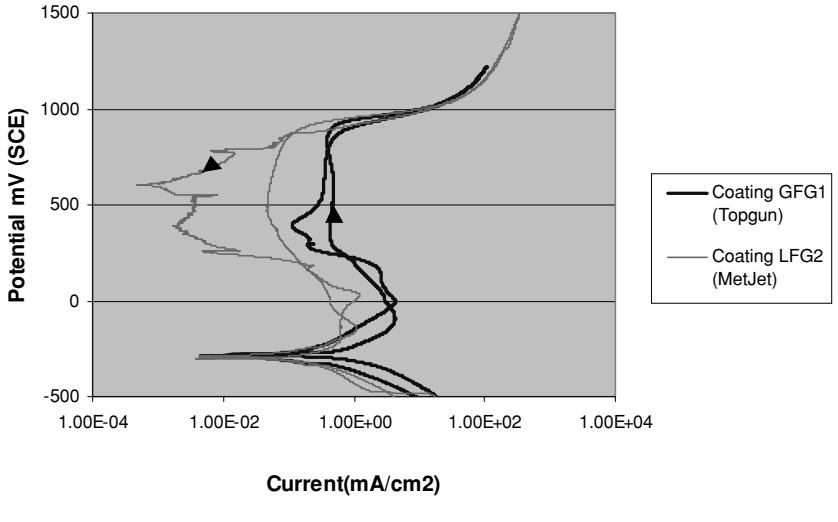

Figure 8 Reversed potentiodynamic plots for the coatings produced by Topgun and MetJet II systems using a gas-atomised powder.

TABLE VII Calculated wt% gas products and flame temperatures after the combustion of propylene and kerosene

Coating type	Type of fuel	Richness in oxygen	Flame temp K	CO_2	CO	H_2O	H_2	OH	H	O_2	O
GFG	Propylene	0.73	3042	15.3	31.9	34	9.8	3.9	3.4	1.2	0.9
GFW	Propylene	0.89	3081	20.8	23.3	34	5.3	6.3	2.8	5	2.1
LFW	Kerosene	1.08	3166	23.8	16	35.2	3.1	7.4	1.1	11.4	2.5

The absence of intra-splat oxides in MetJet II coatings and the lack of oxide forming in flight has also been noted by Dent *et al.* [5]. In Topgun coatings, oxide layers formed in intra- and inter-splat configurations particularly with the use of gas-atomised powder. Inter-splat boundaries were found to exist parallel and perpendicular to the substrate, see Fig. 2a. The perpendicular oxide layers may form due to the presence of greater amounts of melted material in the Topgun coatings. This liquid will allow the oxide layer to form more rapidly and then promote redistribution when the liquid splats onto the substrate. The splat thickness in coatings produced by liquid fuel spraying system is thicker in comparison to the splats obtained from a gaseous fuel system, (compare the splat thickness in Fig. 2a and b, $\sim$20 μm for MetJet II and $<$10 μm for Topgun). Although the particle velocity prior to impact in MetJet II system is greater, the particles do not spread into lenticular splats as it is in the solid or semi-solid state. The kinetic energy possessed by the particle does produce some plastic deformation in the semi-solid and the solid core.

It may be demonstrated that each splat in a MetJet II coating, has to wait approximately a few tenths of a second before the next layer is deposited. This may be compared with an in flight residence time of a few milliseconds, thus allowing more oxide to form on the substrate if temperature and oxidising conditions are suitable. A greater proportion of Topgun spray particles are in the molten state as they spend greater time inflight, thus oxide growth may be more advanced before reaching the substrate. Inflight oxide in Topgun coatings may distribute itself on impact in different orientations as the more numerous splats spread on the substrate.

4.3. Degree of melting

The small amount of molten material in MetJet II coatings relates to the reduced particle residence time in the faster moving hot gas of a liquid fuel HVOF system. An additional effect may arise from the presence of the surface oxide on the original water-atomised powder, which would reduce its thermal conductivity near its surface. This oxidized layer is capable of decreasing the thermal flux to the inner regions by one third if the thermal conductivity of the oxides are considered. This would increase the volume fraction of unmelted material during the spraying of water-atomised powder. With gas-atomised powder the absence of an initial oxide barrier and the limited period of heating produces an optimum amount of melting at the surface of the powder in the MetJet II system. This pattern of partial melting has also been observed with Inconel 625 coatings as produced by a liquid fuel spray gun [12].

With the MetJet II gun the higher level of particle momentum prior to impact may promote a local increase in temperature on the substrate. This may be capable of increasing the amount of melted material and/or plastic deformation on arrival at the substrate. A rise of temperature up to 900°C may be expected locally if the kinetic energy was all converted to thermal energy as nickel powder particles impact at a velocity of 1000 m/s. This energy of impact may encourage local melting and thus improve the coherence of splats particularly in this system.

4.4. Formation of porosity

In Topgun spraying where the majority of powder particles have been melted, shrinkage of the solidified material on the substrate may play a part in forming porosity. Micro-porosity from this source was much more widespread in these gaseous fuel sprayed coatings. In MetJet II coatings there are a few large pores possibly due to the poorer flowability of splats as the amount of liquid phase is small at this stage, see Fig. 5. Thus in MetJet II coatings a smaller volume of molten material is capable of holding particles together but also of reducing the amount of shrinkage due to solidification. Higher velocity particles in the MetJet II spraying process can also promote plastic deformation of the semi-solid and solid core of each particle on impact at the substrate and this may also help to reduce porosity.

The higher level of porosity in coatings produced from water-atomised powders may arise from two factors i.e., the retention of more solid in the particles as the pre-existing oxide acts as a thermal barrier and then the retention of oxide on solid particle surfaces. This will decrease the splat radius and increase the splat thickness. This is consistent with the result obtained from previous investigations [13]. The porosity in gas-atomised Topgun coatings is more widely dispersed, as micro-porosity resulting from shrinkage during solidification of the sprayed liquid droplets. However the level of porosity particularly in the gas-atomised MetJet II coatings is lower, with most of the macro porosity features being removed, see Fig. 2b and the micro-porosity being present close to the splat boundaries, where some melting had occurred and encouraged inter-splat welding. In the case of water atomised MetJet II coatings the pre-existing oxide prevents inter-splat welding on parallel and perpendicular layers and thus allow porosity to exist in both orientations, see Fig. 3.

Water-atomised powder sprayed with the MetJet II system produced the least oxide content but the largest proportion of unmelted particles. This prevented extensive flowability in the splats and promoted higher levels of porosity as demonstrated in coating LFW, see Table III and Fig. 5. This accounts for the 0.4% porosity

for a gas-atomised powder coating (LFG) and the 1.6% for a water-atomised powder coating (LFW). The oxide layer on the powder acts as a thermal barrier, reducing the volume fraction of molten material, thus weakening the adhesion of splats perpendicular to the substrate and allowing the corrodant to percolate the coating and attack the steel. Also the relatively fast deterioration of the water-atomised powder coatings produced by MetJet II system in a salt spray test will directly relate to the presence of such open porosity networks and the first observation of rusting after 3 h. This coating was still able to protect 75% of the steel after 2000 h exposure, suggesting that the initial sites of corrosion were less numerous and have not linked to undermine the coating at a high rate.

A gas-atomised powder coating sprayed by the Topgun system (GFG) showed earlier signs of corrosion in the salt spray test i.e., after 36 h exposure. This reduced level of corrosion resistance may be attributed to the higher level of porosity in coating GFG due to the shrinkage of the melted material in the Topgun system. Degradation of this coating continued so that 80% of the area had been undermined after 2000 h exposure in the salt spray cabinet.

Both Topgun coatings (GFW and GFG) failed within a relative short space of time under salt spray test conditions. The coating (GFW) produced from the water atomised powder underwent 120 h testing before the underlying substrate was attacked whilst the gas atomised powder coating (GFG) experienced 36 h of testing. If porosity is the key issue in controlling corrosion then the early onset would be expected with the GFW coating (4.2% porosity) as opposed to the GFG coating (2.1% porosity). Hence it is not the amount of porosity which matters but the type of porosity i.e., whether or not it is interconnecting. With water atomised powder less melting has occurred with the presence of a pre-oxide, on its surface i.e., the oxide is acting as a thermal barrier. Less melting promoted thicker splats and less opportunity for porosity to exist perpendicular to the substrate interface. This demonstrates the importance of this type of porosity to the initial time to substrate corrosion. The better performance of the GFW coating over the LFW coating in this respect arises from the combination of percentage of powder melted and the retention of the pre-oxide during the spraying of water atomised powder. Additional time in flight and therefore, greater heat transfer encourages more melting and thus the break down of the oxide pre-layer in the GFW coating, Hence, in the LFW case although the opportunity for less perpendicular porosity may exist with minimal melting, the combusted gas stream is not able to break down the pre-oxide and so that the splats do not weld together. The corrodant is able to percolate quickly (3 h) at a relatively small number of sites to the underlying substrate.

The potentiodynamic work demonstrates that there are differences in passivation behaviour between the two forms of coating i.e., liquid fuel and gas fuel sprayed. For the liquid fuel sprayed coating the passivation current is reduced by approaching an order of magnitude indicating either the presence of more stable passive film or less influence from the substrate through inter-connecting porosity. The more stable films could result from less open porosity on the surfaces of the coating which will reduce any local crevice effects. Some effects may result from the presence of preformed oxides in the case of those coatings produced from water atomised powders. Overall the influence of any of the intrinsic corrosion resistance of the coating materials themselves is small when protecting the underlying substrate. The major effect arises from the pattern of defects in the coatings which depend upon the powder characteristics and the conditions employed in the spray process.

5. Conclusion

The influence of the spraying system and the type of powder, on microstructure and aqueous corrosion properties of a Ni-20%Cr HVOF coating can be summarised as follows:

- The greatest corrosion protection to the steel substrate is given by coatings produced from gas-atomised Ni-20%Cr powders when sprayed by the liquid fuelled MetJet II system. These were able to withstand >3000 h exposure in a neutral salt spray test without substrate corrosion. This is two orders of magnitude greater than with gas fuelled coatings (Topgun) produced from the same powder.
- MetJet II spray system produced coatings with a smaller amount of oxide, less porosity and less evidence of melting than is the case with the propylene fuelled Topgun.
- The gas velocity in the MetJet II system is much greater than in Topgun, which increases the transfer of kinetic energy to the powder particles and this reduces residence time in the gas stream and restricts the rise in particle temperature.
- As the injection point of the feedstock powder into the MetJet II system is later i.e., after the combustion chamber, the temperature rise of the powder is at levels below those in the Topgun system.
- The residence time in the combusted gas influences the formation of oxide on the powder, so that in a liquid fuel HVOF gun the amount of oxide is reduced despite the presence of a higher oxygen concentration in the combustion gas stream.
- The distribution and orientation of oxide films and pores has a major role on coating properties e.g., the presence of oxides and pores running perpendicular to the substrate influences aqueous corrosion protection significantly. The amount of molten material in the coating splats controls the distribution pattern of oxide and porosity e.g., in the Topgun coating.
- Water atomised powder produced a higher fraction of unmelted material and porosity together with less oxides than the gas-atomised powder coatings produced by both spraying systems. This relates to the existence of pre-oxide (Cr_2O_3) layer on the water-atomised powder prior to spraying, which may act as a thermal barrier.

Acknowledgement

The authors would like to thank Professor T.H. Hyde, Head of the School of Mechanical, Material, Manufacturing Engineering and Management, University of Nottingham for providing facilities for this work and the Ministry of Science, Research, and Technology in Iran for providing financial support. Our thanks are also extended to Professor D.G. McCartney, Dr. D. Zhang and Dr. A.J. Horlock for advice on the HVOF spraying techniques.

References

1. M. L. THORPE and H. J. RICHTER, in Proceedings of International Thermal Spray Conference (ASM, USA, 1992) p. 137.
2. C. H. CHANGE and R. L. MOORE, in Proceedings of 8th National Thermal Spray Conference (ASM, USA, 1995) p. 207.
3. H. EDRIS, D. G. MCCARTNEY and A.J. STURGEON, *J. Mater. Sci.* **32** (1997) 863
4. G. SAI, PhD thesis, University of Nottingham, September 2000.
5. A. H. DENT, A. J. HORLOCK, S. J. HARRIS and D. G. MCCARTNEY, *Trans IMF* **77** (1999) 60.
6. A. J. STURGEON, in "Thermal Spray 2001: New Surfaces for a New Millennium, ASM, USA," edited by C. C. Berndt, A. K. Khor and E. F. Lugscheider (2001) p. 1149.
7. A. H. DENT, A. J. HORLOCK, S. J. HARRIS and D. G. MCCARTNEY, in Proceeding of the 15th International Thermal Spray Conference, ASM, USA (1998) p. 665.
8. N. BIRKS and G. H. MEIER, Introduction to High Temperature Oxidation of Metals, Edward Arnold, Pittsburgh, 1983.
9. P. KOFSTAD, "High Temperature Oxidation of Metals" (John Wiley & Sons Inc., New York, 1966).
10. N. BIRKS and H. RICKERT, *J. Inst. Metals* **91** (1961–62) 308.
11. G. L. BORMAN and K. W. RAGLAND, "Combustion Engineering" (McGraw-Hill Company, New York, 1998).
12. D. ZHANG, S. J. HARRIS and D. G. MCCARTNEY, *Mater. Sci. and Engin.* A **344** (2003) 45.
13. V. V. SOBOLEV and J. M. GUILEMANY, *J. Thermal Spray Technol* **8** (1999) 523.

Received 15 July 2002
and accepted 7 July 2003